ACS central science

Research Article

Cite This: ACS Cent. Sci. 2018, 4, 63−70

Controlling the Size of Two-Dimensional Polymer Platelets for Water-in-Water Emulsifiers

Maria Inam, Joseph R. Jones, Maria M. Pérez-Madrigal, Maria C. Arno, Andrew P. Dove,* and Rachel K. O'Reilly*

Department of Chemistry, University of Warwick, Gibbet Hill, Coventry, CV4 7AL, United Kingdom

Supporting Information

ABSTRACT: A wide range of biorelevant applications, particularly in pharmaceutical formulations and the food and cosmetic industries, require the stabilization of two water-soluble blended components which would otherwise form incompatible biphasic mixtures. Such water-in-water emulsions can be achieved using Pickering stabilization, where two-dimensional (2D) nanomaterials are particularly effective due to their high surface area. However, control over the shape and size of the 2D nanomaterials is challenging, where it has not yet been possible to examine chemically identical nanostructures with the same thickness but different surface areas to probe the size-effect on emulsion stabilization ability. Hence, the rationale design and realization of the full potential of Pickering water-in-water emulsion stabilization have not yet been achieved. Herein, we report for the first time 2D poly(lactide) platelets with tunable sizes (with varying coronal chemistry) and of uniform shape using a crystallization-driven self-assembly methodology. We have used this series of nanostructures to explore the effect of 2D platelet size and chemistry on the stabilization of a water-in-water emulsion of a poly(ethylene glycol) (PEG)/dextran mixture. We have demonstrated that cationic, zwitterionic, and neutral large platelets (ca. 3.7×10^6 nm^2) all attain smaller droplet sizes and more stable emulsions than their respective smaller platelets (ca. 1.2×10^5 nm^2). This series of 2D platelets of controlled dimensions provides an excellent exemplar system for the investigation of the effect of just the surface area on the potential effectiveness in a particular application.

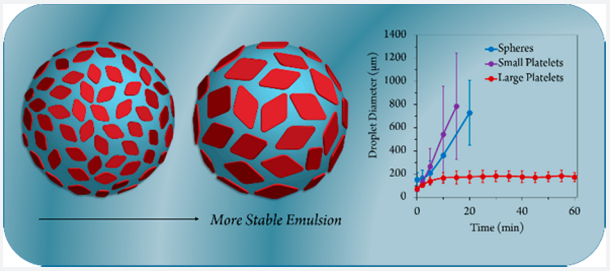

INTRODUCTION

Emulsions of oil and water can be stabilized against coalescence using various emulsifying agents, such as simple surfactants, as they strongly adsorb to oil−water interfaces due to high interfacial tensions. Recently, Pickering emulsions, where the emulsion is stabilized by particles rather than surfactants, have gained increasing interest.[1] Indeed, inorganic colloidal particles, such as silica sols,[2,3] nanocomposites,[4] and Laponite clay platelets,[5−10] as well as organic latexes[11−15] and self-assembled nanoparticles,[16,17] have all been reported as effective stabilizers. Recently, 2D polymer nanostructures, such as amphiphilic[18] and Janus nanosheets,[19] have found application in the formation of Pickering emulsions, although, in these examples, the emulsions are partially stabilized by the amphiphilicity of the particles as well as by a Pickering effect.

A number of applications, particularly in pharmaceutical formulations and the food and cosmetic industries, require stabilization in blending two water-soluble components which would otherwise form incompatible biphasic mixtures. For example, food products contain incompatible water-soluble mixtures such as proteins and polysaccharides.[20] Such blends can be achieved using water-in-water emulsions; however, because of the ultralow interfacial tension and thickness of the interface, stabilization is difficult to accomplish using surfactants.[21,22] Such stabilization can be achieved using triblock copolymers,[23] polymer−protein conjugates,[24] and, recently, elongated and 2D nanoparticle stabilizers have been examined for the stabilization of water-in-water emulsions,[25] where it has been shown that more stable emulsions can be achieved for particles of greater aspect ratio.[26,27] In particular, it was shown that the use of cellulose nanorods[28] and Gibbsite nanoplates can act as efficient emulsifiers.[29] However, these approaches do not offer the ability to readily modulate the chemistry, size, or shape of the construct to explore its effectiveness as a stabilizer. Indeed, despite the recent extensive interest in such ultrathin 2D materials, such as graphene, boron nitride, and clay platelets, for applications in optical devices,[30] catalyst arrays,[31] organic electronics[32] and as templates,[33] investigations into the combination of controlled particle shape and size are much less explored owing to the inability to control this further dimension in inorganic materials. Hence, we propose utilizing the precision and complexity offered by organic polymer assembly methods to create a series of nanoparticle stabilizers of tunable chemistry with controlled size and shape.

A number of techniques exist which focus on the preparation of particles of controlled size and morphology including

Received: September 21, 2017
Published: November 27, 2017

DOI: 10.1021/acscentsci.7b00436
ACS Cent. Sci. 2018, 4, 63−70

Scheme 1. Synthesis of $PLLA_{36}$-*b*-$PDMAEMA_{216}$ and Removal of the RAFT End Group to Produce a Hydrogen-Terminated Polymer before Self-Assembly into Diamond-Shaped Platelets[a]

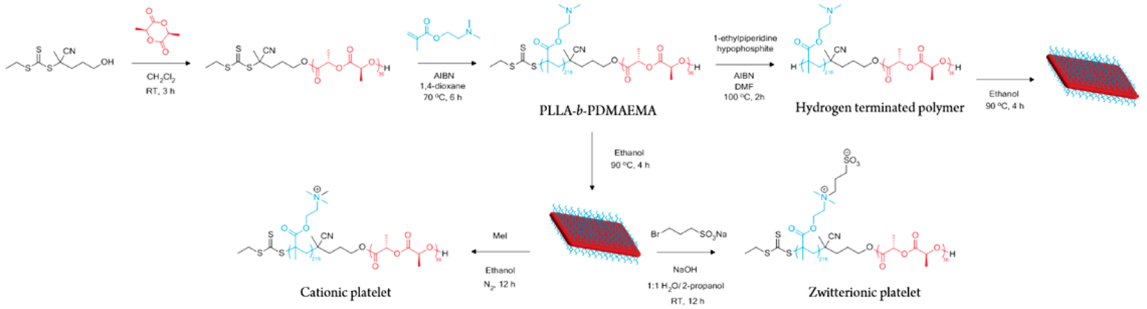

[a]Self-assembly into platelets from $PLLA_{36}$-*b*-$PDMAEMA_{216}$ can also be followed by quaternization with iodomethane to produce cationic platelets and by reaction with bromopropanesulfonic acid to produce zwitterionic platelets.

lithography[34−36] and particle replication in nonwetting template (PRINT) techniques,[37,38] particle stretching,[39−41] and block copolymer self-assembly.[42−44] Crystallization-driven self-assembly (CDSA) methodologies have recently been shown to be useful in preparing 2D nanostructures where the size can be controlled in two dimensions.[45−47] Winnik, Manners, and co-workers reported the use of CDSA methods to prepare a range of 2D assemblies from lenticular to rectangular platelets using a poly(ferrocenyldimethylsilane) core-forming block.[48−52] In these studies and others,[53] size control can be achieved using an epitaxial growth mechanism, with initial formation of disperse assemblies, followed by degradation to produce seed micelles and subsequent controlled growth.[50−52] Polymer platelets using a poly(ε-caprolactone) core-forming block have been studied by Chen,[54,55] Li,[56−58] and Eisenberg[59,60] where the uniformity and shape of the platelets could be tuned, but fine control over the resultant nanoparticle size was somewhat limited.[61] More recently, solvent composition was found to provide morphology and size control in the preparation of polyethylene and polyethylene-*b*-poly(*tert*-butyl acrylate) platelets, giving lenticular crystals of different widths.[62]

Poly(L-lactide) (PLLA) block copolymers have also been studied to some extent. Recently, Wooley and co-workers showed the assembly of cylinders and bundled cylinders using CDSA approaches.[63] Cheng and co-workers also fabricated 2D alternating rings of block copolymer and homopolymer, initially using block copolymer seeds to initiate homopolymer growth and afford 2D PLLA materials.[64,65] We have previously shown that CDSA is possible for various PLLA-containing block copolymers with exclusively cylindrical morphologies obtained with varying block compositions.[66−70] Very recently, we have used $Log P_{oct}$[71,72] to evaluate unimer solubility and exploit a shape selective mechanism toward the formation of smooth diamond-shaped nanoplates.[73] Though the diamond shape of these single crystals is inherent to the PLLA single crystal habit, where the higher rotational symmetry of the orthorhombic unit cell has been correlated with relatively less anisotropic polygonal single crystals,[74] we have previously been unable to control the size of these diamond-shaped crystals or achieve modification of their surface chemistry.

Given the importance of water-in-water emulsions in the food industry, we were keen to further explore such biocompatible PLLA nanoplatelets for use as Pickering emulsifiers, where we can develop the use of CDSA to control the size and shape of the resultant assembly. Indeed, such explorations have not been possible using previously applied nanostructures due to the inaccessibility of suitable nanomaterials. Most significantly, it has not been possible to examine chemically identical nanostructures with the same platelet thickness but different surface areas to independently probe the size-effect on emulsion stabilization ability. Hence, the rationale design and realization of the full potential of Pickering emulsion stabilization of water-in-water emulsions has not yet be fully achieved.

As such, we demonstrate that PLLA platelets of controllable surface area, and identical chemical composition and thickness, can act as effective Pickering emulsifiers for PEG/dextran water-in-water emulsions, where high surface area platelets were found to form more stable emulsions than smaller platelets of lower surface area. We also observed the same trend using platelets with modified coronal chemistries, where we attribute the interfacial stabilization ability to the greater adsorption of high surface area platelets[18] and a restricted rotation ability of such large structures.[19] We expect that the potential of these biocompatible and biodegradable 2D platelets as water-in-water emulsion stabilizers is of high interest on account of the wide applicability of such emulsions in the pharmaceutical,[75] agrochemical, cosmetic and food industries.[76,77] Furthermore, we propose that the ability to prepare such high surface area 2D nanomaterials, of controlled dimensions, now enables the fundamental exploration of the effect of size on their effectiveness in applications such as additives or delivery vehicles.

RESULTS AND DISCUSSION

Synthesis of Diblock Copolymers. On the basis of established synthetic methods, a PLLA macro-CTA was prepared by ring-opening polymerization (ROP) using a dual-functional initiator (Scheme 1).[66,70] Reversible addition−fragmentation chain transfer (RAFT) polymerization was used to prepare a series of block copolymers with a poly(2-dimethylaminoethyl methacrylate) (PDMAEMA) corona block with different block lengths (Table S1). ^{1}H NMR analysis confirmed the theoretical block ratios for each of the diblocks (Figure S1) over the core-to-corona ratio range of 1:1 to 1:9. A clear shift in molecular weight of the monomodal distributions with relatively narrow dispersities was confirmed by SEC refractive index (RI) analysis with good overlap of the UV (λ = 309 nm) trace, showing retention of the RAFT end group (Figure S2).

DOI: 10.1021/acscentsci.7b00436
ACS Cent. Sci. 2018, 4, 63−70

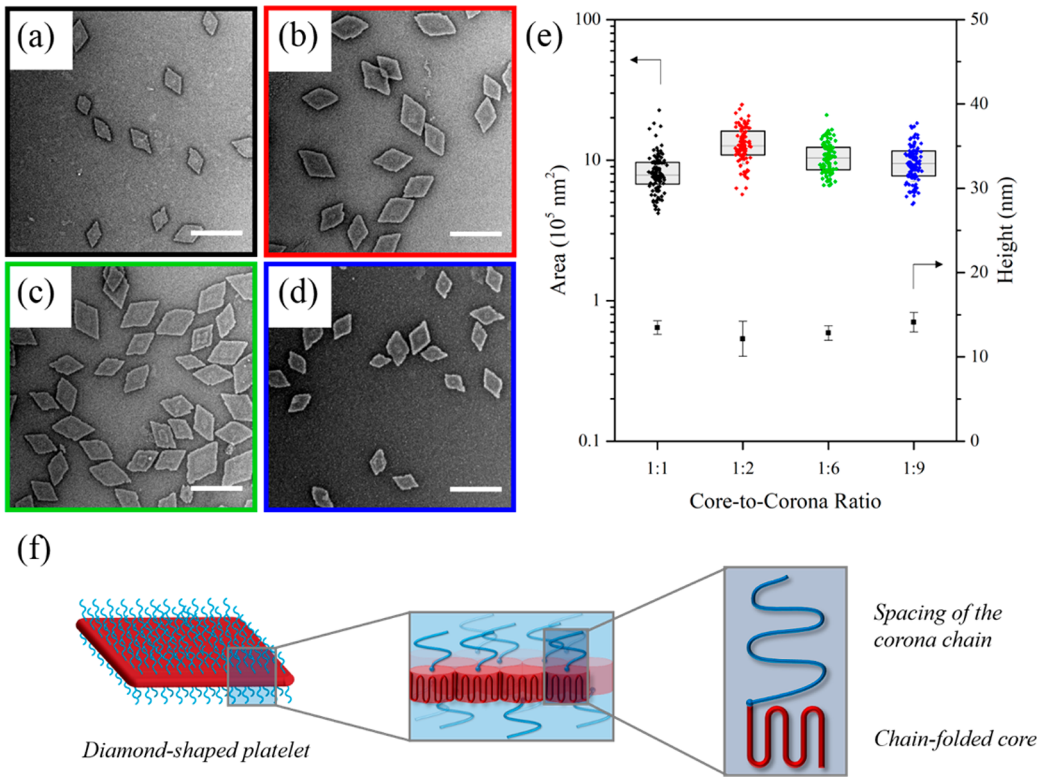

Figure 1. TEM micrographs of (a) PLLA$_{36}$-*b*-PDMAEMA$_{315}$, (b) PLLA$_{36}$-*b*-PDMAEMA$_{216}$, (c) PLLA$_{36}$-*b*-PDMAEMA$_{57}$, and (d) PLLA$_{36}$-*b*-PDMAEMA$_{35}$ diamond platelets. (e) Jitter box plot and average height data showing the negligible difference in area (as determined by TEM) and height of diamond platelets (as determined by AFM) regardless of block ratio. Samples were self-assembled at 90 °C for 4 h, cooled to room temperature, and aged for 1 day. Samples were stained with uranyl acetate. Scale bar = 1 μm. (f) Schematic of a crystallized PLLA-*b*-PDMAEMA polymer chain within a diamond-shaped platelet, showing a representation of the chain-folded core block and the spacing of the corona chain.

Self-Assembly of Diblock Copolymers. For the series of polymers with varying core-to-corona ratio, smooth diamond nanoplatelets were observed after 1 day of aging of a 5 mg mL^{-1} ethanolic solution of diblock copolymer which had been heated for 4 h at 90 °C and then cooled to room temperature (Figure 1). Transmission electron microscopy (TEM) analysis revealed that platelets of uniform size (and hence surface area) were obtained from the self-nucleation of all of the PLLA-*b*-PDMAEMA block copolymers across the composition range investigated (Figure 1, Figure S3), where the zeta potential was measured as ca. + 30 mV for all of the platelets formed (Table S2). Wide-angle X-ray scattering (WAXS) analysis was used to confirm the crystalline nature of the platelets, where a crystalline Bragg peak at 16.6° 2θ was observed, corresponding to the reflections of (110)/(200) planes in the crystalline domains of PLLA (Figure S4). On the basis of literature values, the unit cell of PLLA was reported to be orthorhombic with dimensions of a = 10.683 ± 0.001 Å, b = 6.170 ± 0.001 Å, and c = 28.860 ± 0.004 Å.[78] In comparison to previous work,[65,79,80] atomic force microscopy (AFM) also confirmed no significant difference in the thickness of the collapsed platelet (ca. 12 nm) between different core-to-corona block ratios (Figure S5). Indeed, liquid AFM analysis only suggested a minor difference of ca. 16 nm for the 1:6 ratio block copolymer versus ca. 20 nm for the 1:9 ratio block copolymer, accounting for the increased length of the corona chains (Figure S6).

According to scaling theory by Vilgis and Halperin,[79] a polymer with longer corona chains is expected to form a thinner crystal with more chain-folds (to reduce unfavorable entropic penalties of the overlapping corona chains). In our system, no change in platelet thickness was observed (by dry state AFM measurements) across the series, and static light scattering (SLS) measurements suggested that platelets of the same size and thickness made by blocks of differing core-to-corona ratios have similar aggregation numbers (Figure S7). We hypothesize that the surplus spacing of the corona chain is such that the onset of tethered chain overcrowding has not yet been reached within the range of corona lengths used in this work (Figure 1f).[65] Thus, there is no entropic penalty when increasing the corona block length, and no change in crystal thickness is required.

Notably, these well-defined platelets have been prepared with impressive uniformity without the need for seeded growth methods, which often require carefully controlled concentrations and aging processes. From this result, it is clear that the higher solubility of the PDMAEMA unimers, compared to our previous work primarily using a PDMA coronal block,[73] did not allow for modulation of the number of seeds and hence alteration of the platelet's size. Thus, we deduced that a more significant difference in solubility during the assembly process was required to achieve size control.

Size Control of Diamond Platelets. We then investigated the effect of changing solvent composition for the PLLA$_{36}$-*b*-PDMAEMA$_{216}$ diblock copolymer (1:6 core-to-corona ratio) in order to alter the unimer solubility during the crystallization process. On heating at 90 °C in ethanol, the addition of increasing amounts of tetrahydrofuran (THF) led to an exponential increase in the size of the diamond platelets, regardless of measurement by length or by area (Figure 2,

DOI: 10.1021/acscentsci.7b00436
ACS Cent. Sci. 2018, 4, 63−70

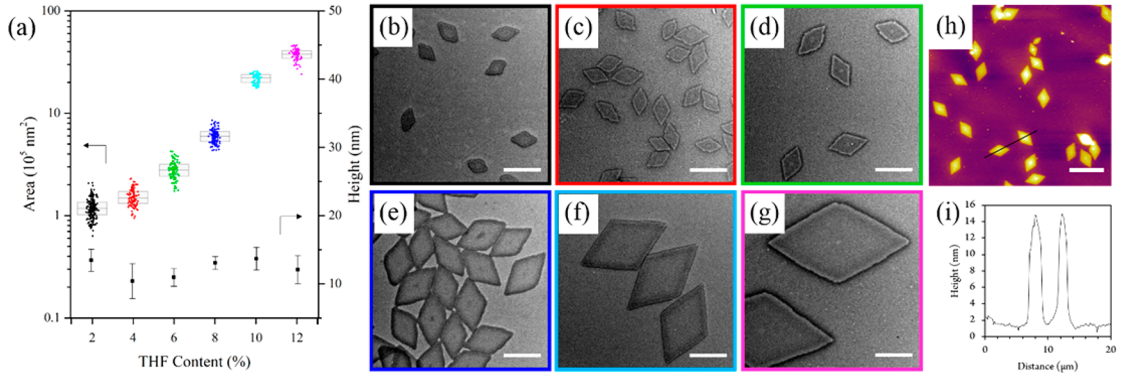

Figure 2. (a) Jitter box plot and average height data showing the exponential increase in $PLLA_{36}$-*b*-$PDMAEMA_{216}$ diamond nanoplatelet area (as determined by TEM) with increasing THF content with a negligible difference in height (as determined by AFM). TEM micrographs of nanoplatelets prepared in ethanol with (b) 2%, (c) 4%, (d) 6%, (e) 8%, (f) 10%, and (g) 12% THF. Scale bar = 1 μm. (h) AFM image and (i) height profile of nanoplatelets prepared with 12% THF. Scale bar = 5 μm. Samples were self-assembled at 90 °C for 4 h and cooled to room temperature. Note that no change in size was observed on prolonged heating of the solutions (Figure S9).

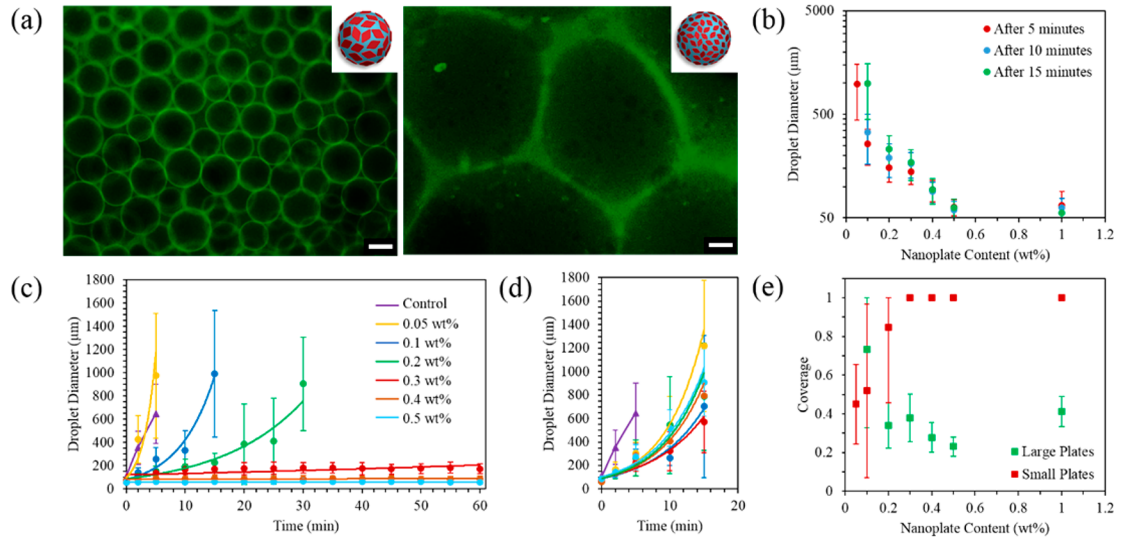

Figure 3. (a) Fluorescence microscopy image of emulsion droplets prepared with large (left) and small (right) diamond platelets after 60 min at 0.5 wt % using 0.01 wt % fluorescein-labeled dextran, where the green color indicates the dextran-rich phase. Scale bar = 200 μm. (b) Plot showing the decrease in emulsion droplet diameter with increasing concentration using large diamond platelets at 5, 10, and 15 min. Emulsion droplet diameter using (c) large diamond platelets (prepared with 12% THF) and (d) small diamond platelets (prepared with 0% THF) as a function of time. (e) Effect of small and large platelets on particle coverage of the droplets. Error bars indicate the standard deviation in droplet diameter when counting ca. 100 droplets.

Figure S8). The difference in size was attributed to increased solubility producing fewer crystalline nuclei, thus leaving more unimers to grow along the crystal front. Furthermore, on increasing the heating time, no change in the size of the platelets was observed, indicating that the assemblies formed are indeed not simply kinetic products, but colloidally stable structures (Figure S9).

AFM analysis showed a consistent height of 12.3 ± 1.7 nm for all of the platelets prepared, typical of a polymer crystal with a single layer of chain folds (Figures 2 and S10). In this work, diamond-shaped platelets of up to ca. 3.75 μm in length were studied in detail; however, it should be noted that the addition of larger amounts of THF (14%) during the assembly process can be used to prepare even larger structures (ca. 9.5 μm in length, Figure S11). Significantly, freeze-dried platelets of all sizes, after removal of ethanol/THF, could be redispersed in water (at concentrations up to 50 mg mL^{-1}) with no observed difference in their size or dispersity. Thus, these platelets in aqueous media were then considered as stabilizers in water-in-water emulsions.

Pickering Emulsions. Given the ability to control the surface area of the $PLLA_{36}$-*b*-$PDMAEMA_{216}$ platelets while maintaining the same chemical composition and the same thickness, we investigated their ability to act as Pickering emulsifiers. Indeed, previous research has indicated that clay and cellulose particles of different shapes have greater potential in stabilizing water-in-water emulsions.[27−29] Herein, we precisely control the size of platelets with the same 2D shape to fully understand their potential to act as a stabilizer.

We used a 5 wt % dextran and 4 wt % PEG mixture as a model system, as this is well-known to phase separate into two macroscopically distinct layers consisting of a dextran-rich phase and a PEG-rich phase, as shown in previously reported phase diagrams,[81] giving an ultralow interfacial tension of ca. 3.05 μN/m.[22] These so-called rich phases, as opposed to pure dextran and pure PEG phases, can be partially accounted for by

DOI: 10.1021/acscentsci.7b00436
ACS Cent. Sci. 2018, 4, 63−70

the inherent high dispersity of the naturally occurring dextran and PEG polymers used; for example, smaller molecular weight dextran polymers are compatible in the PEG phase. Regardless, the water-in-water nature of this system is appropriately stable for the hydrophilic nature of the polymer corona chains present on both sides of the nanoplatelets, where the platelets show no significant preference for the PEG phase or the dextran phase by dynamic light scattering (DLS) measurements (Table S3). Evidence for a PEG in dextran emulsion (where the volume fraction of the dispersed phase is $\varphi = 0.400$) was illustrated using fluorescence microscopy images of emulsions prepared using 0.01% of dextran labeled with fluorescein dye (Figure 3a). It should be noted that a difference in droplet size was observed when using fluorescein-labeled dextran, where all droplet sizes appeared to marginally increase; however, this can be accounted for by the difference in molecular weight exhibited by SEC analysis (Figure S12). Hence, all subsequent measured droplet sizes without the use of fluorescein-labeled dextran are reported here.

To study the effect of platelet size on emulsion stability, the use of small diamond-shaped platelets (ca. 1.2×10^5 nm^2, prepared using 0% THF) and large diamond-shaped platelets (ca. 3.7×10^6 nm^2, prepared using 12% THF) were compared at different concentrations (0.05, 0.1, 0.2, 0.3, 0.4, and 0.5 wt %). At a platelet content of up to 0.3 wt %, emulsions prepared with the small platelets were found to be unstable, where the droplets exhibited a loss of spherical shape with time and increased in size dramatically, with no droplets observed after 20 min. However, emulsions prepared with large platelets at a loading of 0.3 wt % showed a continuously consistent droplet size measured up to 60 min (Figures 3, S13 and S14), with eventual phase separation occurring after ca. 2 days. In a control experiment, emulsions prepared using $PLLA_{36}$-*b*-$PDMAEMA_{216}$ spherical micelles (136 ± 35 nm diameter, 5.4×10^4 nm^2 surface area, Figure S15) also showed a similar lack of stability to that of the small platelets, where the emulsion droplets again increased in size dramatically with phase separation observed after ca. 20 min (Figure S16). Conceptually, it is noteworthy that platelets of greater surface area provide improved stabilization, whereas platelets with a lower surface area, although possessing the same 2D shape, provide a similar lack of stabilization to that of their spherical counterparts.

We can attribute the increased stability to several factors. First, we consider that colloidal particles stabilize the emulsion by lowering the free energy. Given a uniform surface chemistry, the adsorption energy can be given by the following equation:

$$\text{adsorption energy} \propto \frac{1}{\gamma\sigma}$$

where γ is the interfacial tension and σ is the cross-sectional area of a colloidal particle.[3,82] Given that the water−water interface has an ultralow interfacial tension, as previously discussed, the adsorption energy is relatively weak unless σ is sufficiently large enough to prevent coalescence of the droplets by keeping each water phase sufficiently apart. The use of large platelets allows for much larger σ value, thus reducing the free energy of adsorption, without increasing the mass of the particle such that sedimentation of the platelets and subsequent destabilization of the emulsion occur.[29] The larger platelets also provide a greater barrier toward rotation, thus providing a more stable emulsion.[19] Using a droplet relaxation method,[81,83] the emulsion using large platelets also showed a drop in interfacial tension in comparison to the small platelet emulsion, indicating that surface area, and not simply a 2D shape, plays a key role in determining interfacial properties (Table S4, Figures S17 and S18). It should be noted that, previously, small Gibbsite (clay) platelets at similar loading levels were shown to produce more stable emulsions than larger platelets.[29] However, in this case, the large Gibbsite platelets were also of increased thickness (30−40 nm vs. 7 nm), and therefore increased mass, which may account for the resulting destabilization.

Beyond 0.3 wt % of large platelets, the droplet size continued to remain consistent over time, and an increase in concentration only served to reduce the droplet size further, yet the surface coverage of the droplets did not exhibit any significant change (Figure 3e). Notably, the calculated coverage shows that even partial coverage of the emulsion colloids provide good stabilization, in accordance with previous work.[28]

Further attempts to increase the stability using small platelets were also considered, namely, by significantly increasing the loading to 1 wt %, where an even greater total surface area is available to stabilize the emulsion droplets, resulting in a greater than maximum calculated coverage. However, this was also unsuccessful, where no decrease in droplet size was observed despite the high loading of the platelets (Figure S19). This emphasizes the importance of platelet size as opposed to platelet concentration, where a greater total surface area of the small platelets fails to achieve the same stabilization of the emulsion droplets as a lower total surface area of larger platelets. A similar platelet size effect was also observed using a 10 wt % dextran and 2 wt % PEG formulation (Figure S20), where the emulsion was found to be much less stable using small platelets, but exhibited a similar stability with the larger platelets, demonstrating that the small platelets continue to show lower efficiency even with a smaller dispersed phase ($\varphi = 0.200$).

Effect of Changing the Coronal Chemistry. In order to investigate the stabilization of the emulsions further, we sought to monitor the effect of surface chemistry of the platelets. Using the 1:6 core-to-corona ratio block copolymer, modifications were carried out to prepare the equivalent sized platelets with quaternized and zwitterionic chemistries (Scheme 1, as confirmed by ^{1}H NMR analysis and zeta potential measurements, Figures S21 and S22, Table S2). To ensure that the modified corona had no effect on the crystallization of the platelet, both modifications on the small and large platelets (prepared with 0% and 12% THF, respectively) were carried out after assembly, where TEM imaging revealed no noticeable difference in the dimensions of the platelets before and after modification (Figure S23).

At 0.3 wt %, both modifications resulted in lower emulsion stability in comparison to the unmodified platelets; however, the large platelet emulsions still continued to exhibit higher stability and smaller droplet sizes than the corresponding small platelet emulsions (Figure S24), thus further demonstrating that the platelet size (regardless of chemistry) plays a key role in emulsion stability. Noticeably, at 0.5 wt %, the emulsions using quaternized large platelets resulted in a much larger droplet size with phase separation observed after ca. 10 min, whereas the emulsions using zwitterionic large platelets resulted in a comparatively smaller droplet size with phase separation observed after ca. 35 min, though, again, both emulsions were still found to be less stable in comparison to the unmodified platelets (Figure S25). Though a drop in the interfacial tension was observed with the large zwitterionic platelets (Table, S4,

DOI: 10.1021/acscentsci.7b00436
ACS Cent. Sci. 2018, 4, 63−70

Figure S26), the short-term life of the corresponding small platelet emulsion and quaternized platelets did not allow measurement of the interfacial tension using the droplet relaxation method. Indeed, the overall lack of stabilization can be explained by the preference shown by the quaternized and zwitterionic platelets for the dextran phase, as measured by DLS analysis, where the larger structures observed in dextran solution account for the aggregation of the dextran molecules around the dispersed platelets in comparison to the smaller structures observed in PEG solution (Table S3). Indeed, on eventual phase separation, the neutral platelets appear to sit in the PEG-rich phase, whereas the quaternized and zwitterionic platelets sit in the dextran-rich phase (Figure S27).

Given that the more hydrophilic quaternized and zwitterionic platelets preferred the dextran-rich phase, we then investigated the effect of polymer hydrophilicity by removing the RAFT end group to produce a hydrogen-terminated polymer (Scheme 1) with the same corona chemistry as our most effective stabilizer. Using the 1:6 core-to-corona ratio block copolymer, a loss of the UV signal (λ = 309 nm) in SEC measurements confirmed that the end group had been sufficiently removed (Figure S28). A solvent composition of 12% THF in ethanol was used as to prepare large diamond platelets as discussed previously. However, the size of the platelets increased (ca. 5.5 × 10^6 nm^2, Figure S29a), likely as a result of the increased unimer solubility (in removing a small hydrophobic group) leading to improved crystallization. In order to monitor the effect of the coronal chemistry only, the assembly conditions were modified to prepare platelets of a similar size to those discussed previously as "large" platelets. As such, it was found that 10% THF allowed the preparation of diamond-platelets of comparable size (ca. 4.0 × 10^6 nm^2, Figure S29b). Using a 5 wt % dextran and 4 wt % PEG mixture with 0.5 wt % of these platelets to prepare the emulsion, a similar decrease in Pickering stabilization was observed, where the droplet size increased to eventual phase separation after ca. 10 min (Figure S30). Consistent with the zwitterionic and quaternized platelet emulsions, the phase separated emulsion showed the end group removed platelets were present in the dextran-rich phase (Figure S31), thus explaining the overall lack of long-term stabilization with such chemistries. However, regardless of the duration of stabilization, it is especially noteworthy that the size of the platelet plays a key role in its ability to act as an emulsifier, where the use of a larger platelet results in improved stabilization for all of the surface chemistries studied.

CONCLUSIONS

We have successfully demonstrated the formation of uniform 2D diamond-shaped nanoplatelets with a range of different sizes (up to ca. 9.5 μm in length) using biorelevant poly(lactide) block copolymers. We have achieved significant control over their surface area while maintaining a single crystal thickness. Importantly, this can be achieved without modifying the chemistry of the copolymer or its block ratios, but instead using a simple unimer solubility approach, where the addition of "good" solvents can be used to achieve greater unimer solubility and hence allow for the preparation of larger and more perfect single crystal assemblies. This unprecedented control over surface area was exploited in the design of Pickering water-in-water emulsifiers, where we have shown that larger platelets (ca. 3.7 × 10^6 nm^2) attain smaller droplet sizes and more stable emulsions than smaller platelets (ca. 1.2 × 10^5 nm^2) at concentrations as low as 0.3 wt %. We propose that this is due to their large surface area which exhibits greater adsorption properties, and a larger barrier towards rotation of the particles.[18] Though it is noted that stable emulsions can only be prepared when the particles show little preference for either phase, the platelet size-emulsion stability trend was observed across a range of coronal chemistries. This highlights that the ability to control the size of 2D platelets can allow for the design of effective interfacial stabilizers for application in water-in-water emulsions. Such 2D platelets of controlled dimensions and chemistries are expected to find further utilization in the pharmaceutical, agrochemical, green chemistry, cosmetics, and/or food industry.

ASSOCIATED CONTENT

Supporting Information

The Supporting Information is available free of charge on the ACS Publications website at DOI: 10.1021/acscentsci.7b00436.

Experimental details and additional results (PDF)

AUTHOR INFORMATION

Corresponding Authors

*(A.P.D.) E-mail: a.p.dove@warwick.ac.uk.

*(R.K.O.) E-mail: rachel.oreilly@warwick.ac.uk.

ORCID

Andrew P. Dove: 0000-0001-8208-9309

Rachel K. O'Reilly: 0000-0002-1043-7172

Notes

The authors declare no competing financial interest.

ACKNOWLEDGMENTS

The authors thank EPSRC and ERC (Grant No. 615142) and University of Warwick for funding. Zachary Coe is also acknowledged for preparing the Jitter box plots. Jonathan Moffat (Asylum Research, Oxford Instruments) is thanked for liquid AFM measurements, and Daniel Lester (University of Warwick) is acknowledged for SEC measurements of dextran polymers.

ABBREVIATIONS

PLLA, poly(L-lactide); CDSA, crystallization-driven self-assembly; ROP, ring-opening polymerization; RAFT, reversible addition−fragmentation chain-transfer polymerization; PDMAEMA, poly(dimethylaminoethyl methacrylate); THF, tetrahydrofuran; TEM, transmission electron microscopy; AFM, atomic force microscopy; PEG, poly(ethylene glycol); DLS, dynamic light scattering; WAXS, wide-angle X-ray scattering; PRINT, particle replication in nonwetting template; SLS, static light scattering

REFERENCES

(1) Ramsden, W. Separation of Solids in the Surface-Layers of Solutions and Suspensions. *Proc. R. Soc. London* **1903**, *72*, 156−164.

(2) Binks, B. P.; Lumsdon, S. O. Stability of oil-in-water emulsions stabilised by silica particles. *Phys. Chem. Chem. Phys.* **1999**, *1*, 3007−3016.

(3) Levine, S.; Bowen, B. D.; Partridge, S. J. Stabilization of emulsions by fine particles I. Partitioning of particles between continuous phase and oil/water interface. *Colloids Surf.* **1989**, *38*, 325−343.

(4) Fujii, S.; Read, E. S.; Binks, B. P.; Armes, S. P. Stimulus Responsive Emulsifiers Based on Nanocomposite Microgel Particles. *Adv. Mater.* **2005**, *17*, 1014−1018.

DOI: 10.1021/acscentsci.7b00436
ACS Cent. Sci. 2018, 4, 63−70

(5) Ashby, N. P.; Binks, B. P. Pickering emulsions stabilised by Laponite clay particles. *Phys. Chem. Chem. Phys.* **2000**, *2*, 5640−5646.
(6) Nonomura, Y.; Kobayashi, N. Phase inversion of the Pickering emulsions stabilized by plate-shaped clay particles. *J. Colloid Interface Sci.* **2009**, *330*, 463−466.
(7) Cauvin, S.; Colver, P. J.; Bon, S. A. Pickering stabilized miniemulsion polymerization: preparation of clay armored latexes. *Macromolecules* **2005**, *38*, 7887−7889.
(8) Bon, S. A.; Colver, P. J. Pickering miniemulsion polymerization using laponite clay as a stabilizer. *Langmuir* **2007**, *23*, 8316−8322.
(9) Cui, Y.; Threlfall, M.; van Duijneveldt, J. S. Optimizing organoclay stabilized Pickering emulsions. *J. Colloid Interface Sci.* **2011**, *356*, 665−671.
(10) Cui, Y.; van Duijneveldt, J. S. Microcapsules composed of cross-linked organoclay. *Langmuir* **2012**, *28*, 1753−1757.
(11) Dinsmore, A.; Hsu, M. F.; Nikolaides, M.; Marquez, M.; Bausch, A.; Weitz, D. Colloidosomes: selectively permeable capsules composed of colloidal particles. *Science* **2002**, *298*, 1006−1009.
(12) Amalvy, J.; Armes, S.; Binks, B.; Rodrigues, J.; Unali, G. Use of sterically-stabilised polystyrene latex particles as a pH-responsive particulate emulsifier to prepare surfactant-free oil-in-water emulsions. *Chem. Commun.* **2003**, 1826−1827.
(13) Gautier, F.; Destribats, M.; Perrier-Cornet, R.; Dechézelles, J.-F.; Giermanska, J.; Héroguez, V.; Ravaine, S.; Leal-Calderon, F.; Schmitt, V. Pickering emulsions with stimulable particles: from highly-to weakly-covered interfaces. *Phys. Chem. Chem. Phys.* **2007**, *9*, 6455−6462.
(14) Binks, B. P.; Lumsdon, S. O. Pickering emulsions stabilized by monodisperse latex particles: effects of particle size. *Langmuir* **2001**, *17*, 4540−4547.
(15) Thompson, K.; Armes, S.; York, D.; Burdis, J. Synthesis of sterically-stabilized latexes using well-defined poly (glycerol monomethacrylate) macromonomers. *Macromolecules* **2010**, *43*, 2169−2177.
(16) Fujii, S.; Cai, Y.; Weaver, J. V. M; Armes, S. P. Syntheses of shell cross-linked micelles using acidic ABC triblock copolymers and their application as pH-responsive particulate emulsifiers. *J. Am. Chem. Soc.* **2005**, *127* (127), 7304−7305.
(17) Mable, C.; Thompson, K.; Derry, M.; Mykhaylyk, O.; Binks, B.; Armes, S. ABC Triblock Copolymer Worms: Synthesis, Characterization, and Evaluation as Pickering Emulsifiers for Millimeter-Sized Droplets. *Macromolecules* **2016**, *49*, 7897−7907.
(18) Mejia, A. F.; Diaz, A.; Pullela, S.; Chang, Y.-W.; Simonetty, M.; Carpenter, C.; Batteas, J. D.; Mannan, M. S.; Clearfield, A.; Cheng, Z. Pickering emulsions stabilized by amphiphilic nano-sheets. *Soft Matter* **2012**, *8*, 10245−10253.
(19) Liang, F.; Shen, K.; Qu, X.; Zhang, C.; Wang, Q.; Li, J.; Liu, J.; Yang, Z. Inorganic janus nanosheets. *Angew. Chem., Int. Ed.* **2011**, *50*, 2379−2382.
(20) Capron, I.; Costeux, S.; Djabourov, M. Water in water emulsions: phase separation and rheology of biopolymer solutions. *Rheol. Acta* **2001**, *40*, 441−456.
(21) Broseta, D.; Leibler, L.; Ould Kaddour, L.; Strazielle, C. A theoretical and experimental study of interfacial tension of immiscible polymer blends in solution. *J. Chem. Phys.* **1987**, *87*, 7248−7256.
(22) Ryden, J.; Albertsson, P.-a. Interfacial tension of dextran—polyethylene glycol—water two—phase systems. *J. Colloid Interface Sci.* **1971**, *37*, 219−222.
(23) Buzza, D. M. A.; Fletcher, P. D.; Georgiou, T. K.; Ghasdian, N. Water-in-Water Emulsions Based on Incompatible Polymers and Stabilized by Triblock Copolymers−Templated Polymersomes. *Langmuir* **2013**, *29*, 14804−14814.
(24) Xue, L.-H.; Xie, C.-Y.; Meng, S.-X.; Bai, R.-X.; Yang, X.; Wang, Y.; Wang, S.; Binks, B. P.; Guo, T.; Meng, T. Polymer−Protein Conjugate Particles with Biocatalytic Activity for Stabilization of Water-in-Water Emulsions. *ACS Macro Lett.* **2017**, *6*, 679−683.
(25) Nicolai, T.; Murray, B. Particle stabilized water in water emulsions. *Food Hydrocolloids* **2017**, *68*, 157−163.
(26) Madivala, B.; Vandebril, S.; Fransaer, J.; Vermant, J. Exploiting particle shape in solid stabilized emulsions. *Soft Matter* **2009**, *5*, 1717−1727.
(27) Kalashnikova, I.; Bizot, H.; Bertoncini, P.; Cathala, B.; Capron, I. Cellulosic nanorods of various aspect ratios for oil in water Pickering emulsions. *Soft Matter* **2013**, *9*, 952−959.
(28) Peddireddy, K. R.; Nicolai, T.; Benyahia, L.; Capron, I. Stabilization of Water-in-Water Emulsions by Nanorods. *ACS Macro Lett.* **2016**, *5*, 283−286.
(29) Vis, M.; Opdam, J.; van't Oor, I. S.; Soligno, G.; van Roij, R.; Tromp, R. H.; Erné, B. H. Water-in-Water Emulsions Stabilized by Nanoplates. *ACS Macro Lett.* **2015**, *4*, 965−968.
(30) Matsui, J.; Mitsuishi, M.; Aoki, A.; Miyashita, T. Molecular optical gating devices based on polymer nanosheets assemblies. *J. Am. Chem. Soc.* **2004**, *126*, 3708−3709.
(31) Zhong, Y.; Wang, Z.; Zhang, R.; Bai, F.; Wu, H.; Haddad, R.; Fan, H. Interfacial self-assembly driven formation of hierarchically structured nanocrystals with photocatalytic activity. *ACS Nano* **2014**, *8*, 827−833.
(32) Wakahara, T.; D'Angelo, P.; Miyazawa, K. i.; Nemoto, Y.; Ito, O.; Tanigaki, N.; Bradley, D. D.; Anthopoulos, T. D. Fullerene/cobalt porphyrin hybrid nanosheets with ambipolar charge transporting characteristics. *J. Am. Chem. Soc.* **2012**, *134*, 7204−7206.
(33) McGrath, N.; Patil, A. J.; Watson, S.; Horrocks, B. R.; Faul, C. F.; Houlton, A.; Winnik, M. A.; Mann, S.; Manners, I. Conductive, Monodisperse Polyaniline Nanofibers of Controlled Length Using Well Defined Cylindrical Block Copolymer Micelles as Templates. *Chem. - Eur. J.* **2013**, *19*, 13030−13039.
(34) Xu, S.; Nie, Z.; Seo, M.; Lewis, P.; Kumacheva, E.; Stone, H. A.; Garstecki, P.; Weibel, D. B.; Gitlin, I.; Whitesides, G. M. Generation of monodisperse particles by using microfluidics: control over size, shape, and composition. *Angew. Chem.* **2005**, *117*, 734−738.
(35) Dendukuri, D.; Pregibon, D. C.; Collins, J.; Hatton, T. A.; Doyle, P. S. Continuous-flow lithography for high-throughput microparticle synthesis. *Nat. Mater.* **2006**, *5*, 365−369.
(36) Rolland, J. P.; Maynor, B. W.; Euliss, L. E.; Exner, A. E.; Denison, G. M.; DeSimone, J. M. Direct fabrication and harvesting of monodisperse, shape-specific nanobiomaterials. *J. Am. Chem. Soc.* **2005**, *127*, 10096−10100.
(37) Kersey, F. R.; Merkel, T. J.; Perry, J. L.; Napier, M. E.; DeSimone, J. M. The effect of aspect ratio and deformability on nanoparticle extravasation through nanopores. *Langmuir* **2012**, *28*, 8773−8781.
(38) Gratton, S. E.; Ropp, P. A.; Pohlhaus, P. D.; Luft, J. C.; Madden, V. J.; Napier, M. E.; DeSimone, J. M. The effect of particle design on cellular internalization pathways. *Proc. Natl. Acad. Sci. U. S. A.* **2008**, *105*, 11613−11618.
(39) Ho, C.; Keller, A.; Odell, J.; Ottewill, R. Preparation of monodisperse ellipsoidal polystyrene particles. *Colloid Polym. Sci.* **1993**, *271*, 469−479.
(40) Champion, J. A.; Katare, Y. K.; Mitragotri, S. Making polymeric micro-and nanoparticles of complex shapes. *Proc. Natl. Acad. Sci. U. S. A.* **2007**, *104*, 11901−11904.
(41) Yoo, J.-W.; Mitragotri, S. Polymer particles that switch shape in response to a stimulus. *Proc. Natl. Acad. Sci. U. S. A.* **2010**, *107*, 11205−11210.
(42) Chen, C.; Wylie, R. A.; Klinger, D.; Connal, L. A. Shape Control of Soft Nanoparticles and Their Assemblies. *Chem. Mater.* **2017**, *29*, 1918−1945.
(43) Elsabahy, M.; Wooley, K. L. Design of polymeric nanoparticles for biomedical delivery applications. *Chem. Soc. Rev.* **2012**, *41*, 2545−2561.
(44) Williford, J.-M.; Santos, J. L.; Shyam, R.; Mao, H.-Q. Shape control in engineering of polymeric nanoparticles for therapeutic delivery. *Biomater. Sci.* **2015**, *3*, 894−907.
(45) Crassous, J. J.; Schurtenberger, P.; Ballauff, M.; Mihut, A. M. Design of block copolymer micelles via crystallization. *Polymer* **2015**, *62*, A1−A13.

DOI: 10.1021/acscentsci.7b00436
ACS Cent. Sci. 2018, 4, 63−70

(46) He, W.-N.; Xu, J.-T. Crystallization assisted self-assembly of semicrystalline block copolymers. *Prog. Polym. Sci.* **2012**, *37*, 1350−1400.
(47) Tritschler, U.; Pearce, S.; Gwyther, J.; Whittell, G. R.; Manners, I. 50th Anniversary Perspective: Functional Nanoparticles from the Solution Self-Assembly of Block Copolymers. *Macromolecules* **2017**, *50*, 3439−3463.
(48) Mohd Yusoff, S. F.; Hsiao, M.-S.; Schacher, F. H.; Winnik, M. A.; Manners, I. Formation of lenticular platelet micelles via the interplay of crystallization and chain stretching: solution self-assembly of poly (ferrocenyldimethylsilane)-block-poly (2-vinylpyridine) with a crystallizable core-forming metalloblock. *Macromolecules* **2012**, *45*, 3883−3891.
(49) Molev, G.; Lu, Y.; Kim, K. S.; Majdalani, I. C.; Guerin, G.; Petrov, S.; Walker, G.; Manners, I.; Winnik, M. A. Organometallic−polypeptide diblock copolymers: synthesis by Diels−Alder coupling and crystallization-driven self-assembly to uniform truncated elliptical lamellae. *Macromolecules* **2014**, *47*, 2604−2615.
(50) Presa Soto, A.; Gilroy, J. B.; Winnik, M. A.; Manners, I. Pointed Oval Shaped Micelles from Crystalline-Coil Block Copolymers by Crystallization Driven Living Self Assembly. *Angew. Chem., Int. Ed.* **2010**, *49*, 8220−8223.
(51) Hudson, Z. M.; Boott, C. E.; Robinson, M. E.; Rupar, P. A.; Winnik, M. A.; Manners, I. Tailored hierarchical micelle architectures using living crystallization-driven self-assembly in two dimensions. *Nat. Chem.* **2014**, *6*, 893−898.
(52) Qiu, H.; Gao, Y.; Boott, C. E.; Gould, O. E.; Harniman, R. L.; Miles, M. J.; Webb, S. E.; Winnik, M. A.; Manners, I. Uniform patchy and hollow rectangular platelet micelles from crystallizable polymer blends. *Science* **2016**, *352*, 697−701.
(53) Yu, B.; Jiang, X.; Yin, J. Size-tunable nanosheets by the crystallization-driven 2D self-assembly of hyperbranched poly (ether amine). *Macromolecules* **2014**, *47*, 4761−4768.
(54) Wang, J.; Zhu, W.; Peng, B.; Chen, Y. A facile way to prepare crystalline platelets of block copolymers by crystallization-driven self-assembly. *Polymer* **2013**, *54*, 6760−6767.
(55) Zhu, W.; Peng, B.; Wang, J.; Zhang, K.; Liu, L.; Chen, Y. Bamboo Leaf-Like Micro-Nano Sheets Self-Assembled by Block Copolymers as Wafers for Cells. *Macromol. Biosci.* **2014**, *14*, 1764−1770.
(56) Li, B.; Wang, B.; Ferrier, R. C., Jr; Li, C. Y. Programmable nanoparticle assembly via polymer single crystals. *Macromolecules* **2009**, *42*, 9394−9399.
(57) Dong, B.; Zhou, T.; Zhang, H.; Li, C. Y. Directed self-assembly of nanoparticles for nanomotors. *ACS Nano* **2013**, *7*, 5192−5198.
(58) Qi, H.; Zhou, T.; Mei, S.; Chen, X.; Li, C. Y. Responsive Shape Change of Sub-5 nm Thin, Janus Polymer Nanoplates. *ACS Macro Lett.* **2016**, *5*, 651−655.
(59) Rizis, G.; van de Ven, T. G.; Eisenberg, A. Raft" Formation by Two-Dimensional Self-Assembly of Block Copolymer Rod Micelles in Aqueous Solution. *Angew. Chem., Int. Ed.* **2014**, *53*, 9000−9003.
(60) Rizis, G.; van de Ven, T. G.; Eisenberg, A. Homopolymers as structure-driving agents in semicrystalline block copolymer micelles. *ACS Nano* **2015**, *9*, 3627−3640.
(61) Su, M.; Huang, H.; Ma, X.; Wang, Q.; Su, Z. Poly (2-vinylpyridine)-block-Poly (ϵ-caprolactone) Single Crystals in Micellar Solution. *Macromol. Rapid Commun.* **2013**, *34*, 1067−1071.
(62) Fan, B.; Wang, R.-Y.; Wang, X.-Y.; Xu, J.-T.; Du, B.-Y.; Fan, Z.-Q. Crystallization-Driven Co-Assembly of Micrometric Polymer Hybrid Single Crystals and Nanometric Crystalline Micelles. *Macromolecules* **2017**, *50*, 2006−2015.
(63) Song, Y.; Chen, Y.; Su, L.; Li, R.; Letteri, R. A.; Wooley, K. L. Crystallization-driven assembly of fully degradable, natural product-based poly (l-lactide)-block-poly (α-d-glucose carbonate) s in aqueous solution. *Polymer* **2017**, *122*, 270−279.
(64) Chen, W. Y.; Li, C. Y.; Zheng, J. X.; Huang, P.; Zhu, L.; Ge, Q.; Quirk, R. P.; Lotz, B.; Deng, L.; Wu, C.; Thomas, E. L.; Cheng, S. Z. D. " Chemically shielded" poly (ethylene oxide) single crystal growth and construction of channel-wire arrays with chemical and geometric recognitions on a submicrometer scale. *Macromolecules* **2004**, *37*, 5292−5299.
(65) Zheng, J. X.; Xiong, H.; Chen, W. Y.; Lee, K.; Van Horn, R. M.; Quirk, R. P.; Lotz, B.; Thomas, E. L.; Shi, A.-C.; Cheng, S. Z. D. Onsets of Tethered Chain Overcrowding and Highly Stretched Brush Regime via Crystalline− Amorphous Diblock Copolymers. *Macromolecules* **2006**, *39*, 641−650.
(66) Petzetakis, N.; Dove, A. P.; O'Reilly, R. K. Cylindrical micelles from the living crystallization-driven self-assembly of poly (lactide)-containing block copolymers. *Chem. Sci.* **2011**, *2*, 955−960.
(67) Petzetakis, N.; Walker, D.; Dove, A. P.; O'Reilly, R. K. Crystallization-driven sphere-to-rod transition of poly (lactide)-b-poly (acrylic acid) diblock copolymers: mechanism and kinetics. *Soft Matter* **2012**, *8*, 7408−7414.
(68) Sun, L.; Pitto-Barry, A.; Kirby, N.; Schiller, T. L.; Sanchez, A. M.; Dyson, M. A.; Sloan, J.; Wilson, N. R.; O'Reilly, R. K.; Dove, A. P. Structural reorganization of cylindrical nanoparticles triggered by polylactide stereocomplexation. *Nat. Commun.* **2014**, *5*, 5746−5754.
(69) Pitto-Barry, A.; Kirby, N.; Dove, A. P.; O'Reilly, R. K. Expanding the scope of the crystallization-driven self-assembly of polylactide-containing polymers. *Polym. Chem.* **2014**, *5*, 1427−1436.
(70) Sun, L.; Petzetakis, N.; Pitto-Barry, A.; Schiller, T. L.; Kirby, N.; Keddie, D. J.; Boyd, B. J.; O'Reilly, R. K.; Dove, A. P. Tuning the size of cylindrical micelles from poly (L-lactide)-b-poly (acrylic acid) diblock copolymers based on crystallization-driven self-assembly. *Macromolecules* **2013**, *46*, 9074−9082.
(71) Dakshinamoorthy, D.; Weinstock, A. K.; Damodaran, K.; Iwig, D. F.; Mathers, R. T. Diglycerol-Based Polyesters: Melt Polymerization with Hydrophobic Anhydrides. *ChemSusChem* **2014**, *7*, 2923−2929.
(72) Magenau, A. J.; Richards, J. A.; Pasquinelli, M. A.; Savin, D. A.; Mathers, R. T. Systematic Insights from Medicinal Chemistry To Discern the Nature of Polymer Hydrophobicity. *Macromolecules* **2015**, *48*, 7230−7236.
(73) Inam, M.; Cambridge, G.; Pitto-Barry, A.; Laker, Z. P.; Wilson, N. R.; Mathers, R. T.; Dove, A. P.; O'Reilly, R. K. 1D vs. 2D shape selectivity in the crystallization-driven self-assembly of polylactide block copolymers. *Chem. Sci.* **2017**, *8*, 4223−4230.
(74) Cheng, S. Z.; Lotz, B. Nucleation control in polymer crystallization: structural and morphological probes in different length−and time−scales for selection processes. *Philos. Trans. R. Soc., A* **2003**, *361*, 517−537.
(75) Keating, C. D. Aqueous phase separation as a possible route to compartmentalization of biological molecules. *Acc. Chem. Res.* **2012**, *45*, 2114−2124.
(76) Berton-Carabin, C. C.; Schroën, K. Pickering emulsions for food applications: background, trends, and challenges. *Annu. Rev. Food Sci. Technol.* **2015**, *6*, 263−297.
(77) Frith, W. J. Mixed biopolymer aqueous solutions−phase behaviour and rheology. *Adv. Colloid Interface Sci.* **2010**, *161*, 48−60.
(78) Wasanasuk, K.; Tashiro, K.; Hanesaka, M.; Ohhara, T.; Kurihara, K.; Kuroki, R.; Tamada, T.; Ozeki, T.; Kanamoto, T. Crystal structure analysis of poly (l-lactic acid) α form on the basis of the 2-dimensional wide-angle synchrotron X-ray and neutron diffraction measurements. *Macromolecules* **2011**, *44*, 6441−6452.
(79) Vilgis, T.; Halperin, A. Aggregation of coil-crystalline block copolymers: equilibrium crystallization. *Macromolecules* **1991**, *24*, 2090−2095.
(80) Lin, E. K.; Gast, A. P. Semicrystalline diblock copolymer platelets in dilute solution. *Macromolecules* **1996**, *29*, 4432−4441.
(81) Balakrishnan, G.; Nicolai, T.; Benyahia, L.; Durand, D. Particles trapped at the droplet interface in water-in-water emulsions. *Langmuir* **2012**, *28*, 5921−5926.
(82) Sacanna, S.; Kegel, W.; Philipse, A. Thermodynamically stable pickering emulsions. *Phys. Rev. Lett.* **2007**, *98*, 158301−158304.
(83) Ganley, W. J.; Ryan, P. T.; van Duijneveldt, J. S. Stabilisation of Water-in-Water Emulsions by Montmorillonite Platelets. *J. Colloid Interface Sci.* **2017**, *505*, 139−147.

DOI: 10.1021/acscentsci.7b00436
ACS Cent. Sci. 2018, 4, 63−70